Modeling of a permanent-magnet excited synchronous machine with bearing damage

Christelle Piantsop Mbo'o and Kay Hameyer
Institute of Electrical Machines (IEM)
www.iem.rwth-aachen.de
RWTH Aachen University
Schinkelstrasse 4, 52062 Aachen, Germany
Email: christelle.piantsop@iem.rwth-aachen.de

***Abstract*—The detection of bearing damage using the stator current analysis is an important issue in condition monitoring. The modeling of a bearing damage can help to generate data for different loads and faults. These simulation data can be used to develop fault detection and classification algorithms.**
The aim of this work is to develop a model for the bearing damage effects, which enables the simulation of local bearing damage with different sizes. This model is integrated in the model of the permanent-magnet synchronous machine (PMSM) in order to illustrate the impact of the damage on the stator current. Experiments confirm the simulations results of the proposed approach.

***Keywords*—bearing damage, fault modeling, stator current, permanent-magnet synchronous machine**

I. Introduction

The most common mechanical faults in electric drive train are related to bearing damage [1], [2]. These are detected essentially by vibration analysis with different methods for feature extraction [3]. The vibration analysis is expensive compared to other common methods such as temperature monitoring and oil degradation monitoring. However, it is still the most efficient approach, which enables the detection and the location of the failure. This method requires a challenging mechanical construction depending on the number of used accelerometers and the type of bearing. Therefore, an alternative detection method is studied by [4]–[12], where the stator current signature is used for the fault detection. For this reason, the modeling of bearing faults in order to determine their effects on the stator current has become an important issue in condition monitoring. Bearing damage can be modeled considering the vibrations due to the faults ([4], [14]) or the induced torque pulsations ([12], [13]). While, A. Rezig has proposed a model for the vibration of the shaft with bearing damage [14], in which the induced waviness was expressed as a superposition of cosine functions plus the radius of the affected part of the bearing. R. R. Schoen has considered the characteristic fault frequencies generated from the mechanical vibrations [4]. Based on this knowledge, M. Blödt [10] and J. Kim [13] have introduced a model of bearing damage considering the effect of the torque pulsations on the rotor speed, the airgap flux density and the stator current. The torque pulsations was thereby modeled as an additional sinusoidal component with the fundamental fault frequency. In this paper, we focus on the torque pulsations, in such a way that any outer race fault with different width can be represented. The proposed approach can also be applied to other fault types.

The following section describes the dynamic model of the PMSM. Section III introduces the dynamic model of the PMSM with bearing damage, whereas a mathematical expression to describe the torque pulsations due to the bearing damage is discussed in Section III-A. The developed model is simulated for different loads and the results are presented in section IV-A. Furthermore, measurements are shown in order to verify the proposed approach in section IV-B. Finally, the work is summarized and concluded in section V.

II. Dynamic model of the PMSM

A vector controlled PMSM is used for this study. The existing machine model is briefly presented in the following. The dynamic model of the machine can be described in the following equations [16]:

$$v_{sd} = R_s \cdot i_{sd} + L_{sd}\frac{d}{dt}i_{sd} - \omega L_{sq} \cdot i_{sq} \tag{1}$$

$$v_{sq} = R_s \cdot i_{sq} + L_{sq}\frac{d}{dt}i_{sq} + \omega L_{sd} \cdot i_{sd} + \omega \Psi_{PM} \tag{2}$$

where

- v_{sd}, v_{sq}: direct and quadrature stator voltage
- i_{sd}, i_{sq}: direct and quadrature stator current
- L_{sd}, L_{sq}: direct and quadrature inductance
- Ψ_{PM}: flux linkage of the permanent magnet
- R_s stator resistance and ω rotational speed.

The torque of the machine is given by:

$$T_{el} = \frac{3}{2}p \cdot [\Psi_{PM} + (L_{sd} - L_{sq}) \cdot i_{sd}] \cdot i_{sq}. \tag{3}$$

This can also be expressed as the sum of the load torque T_{load} and the moment of inertia J,

$$T_{el}(t) = T_{load}(t) + J \cdot \frac{d}{dt}\omega(t). \tag{4}$$

The model of the controlled PMSM (Fig. 1) based on (1) - (3) is implemented in Matlab/Simulink and consists of three subsystems. The controller is implemented in subsystem *Control Circuit*. The *Power Converter* is modeled in Matlab/PLECS and the machine equations are implemented in subsystem

PMSM. The model input values are the specified speed ω_{spec} and load torque T_{load}. The stator current and the torque of the machine are saved to the workspace for the post-processing in order to evaluate the implemented model.

III. Dynamic Model of the PMSM with Bearing Damage

The dynamic model of the PMSM will be extended with a bearing damage model by modifying the load torque. Thereby, the torque pulsations due to bearing damage have to be implemented and integrated in the whole model.

A. Modeling of the torque pulsations

Local or single-point bearing damage can be classified in function of the affected part of the bearing as inner race fault, outer race fault, cage fault or ball fault. In this paper, we are focussing on the investigation of outer race fault. However, the proposed approach is not restricted to this fault and can also be applied to other fault types. The outer race defect can be modeled by means of the characteristic fault frequencies generated from the mechanical vibrations. These depend on the geometry of the rolling elements and the mechanical rotational frequency f_{rm} and are defined in [15] as:

$$f_{outer} = \frac{N_{ball}}{2} \cdot f_{rm} \cdot (1 - \frac{D_{ball}}{D_{cage}} \cos\beta). \tag{5}$$

N_{ball} represents the number of balls or cylindrical rollers, β the contact angle of the balls, D_{ball} the ball or roller diameter and D_{cage} the cage diameter, also known as the ball or roller pitch diameter. Rolling bearings are usually used to guide and to support the shaft in rotating machines. Any bearing damage causes a radial motion between the rotor and the stator, which leads to a rise of the friction torque in load case. This interferes with the load torque and leads to torque pulsations. In order to model the bearing damage, a mathematical expression must be found to describe the torque pulsations in such a way that outer race fault with different width should be modeled. For this reason, we assume that every time when a ball passes through the damaged point, a disturbance occurs and overlays the load torque. This disturbance can be modeled as a rectangular pulse, whose width depends on the width of the damage and whose amplitude is related to the weighting of the damage. The generated torque pulsation, shown in Fig. 2, can be defined as:

$$T_{dist}(t) = A_{dist} \sum_{k=0}^{\infty} rect\left(\frac{t - \frac{\Delta_{dist}}{2} - k \cdot T_{rect}}{\Delta_{dist}}\right) \tag{6}$$

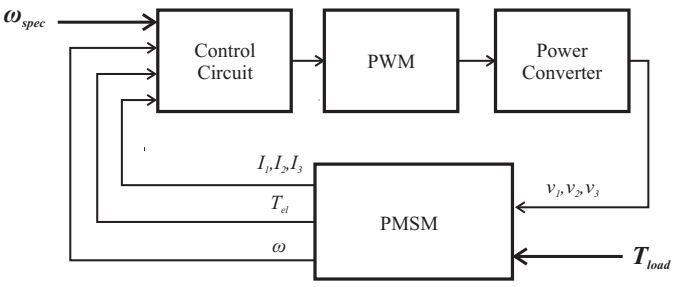

Fig. 1. Dynamic model of the PMSM.

where

- A_{dist} is the amplitude of the disturbing torque related to the bearing damage
- Δ_{dist} is the time, in which a ball passes through the damaged point.
- T_{rect} is the period of the pulse.

Δ_{dist} is calculated by the width of the fault d and the tangential speed of the outer race v_T, which can be expressed as a function of the rotational speed of the cage ω_C and the raceway groove radius r_a [18]:

$$\Delta_{dist} = \frac{d}{v_T} \tag{7}$$

with

$$v_T = \omega_C \cdot r_a = \frac{n_C}{60} \cdot 2\pi \cdot r_a. \tag{8}$$

The period of the pulse T_{rect} depends on how many times the ball crosses over the damaged point inside a motor revolution N_{outer}:

$$T_{rect} = \frac{T}{N_{outer}}, \tag{9}$$

where $T = 1/n$ is the period of the rotational movement and n the rotational speed. N_{outer} is given by the characteristic frequency of the outer race fault from (5) as:

$$N_{outer} = \frac{N_{ball}}{2} \cdot \left(1 - \frac{D_{ball}}{D_{cage}} \cos\beta\right). \tag{10}$$

B. Extended model

The developed approach to represent the bearing damage from section III-A is integrated in the model of the PMSM. Thereby, the load torque of the machine T_{load} is replaced by the load torque with disturbance $T_{load,dist}$, which is the sum of the load torque T_{load} and the disturbing torque T_{dist} from (6):

$$T_{load,dist}(t) = T_{load}(t) + T_{dist}(t) \tag{11}$$

$$T_{load,dist}(t) = T_{load}(t) + A_{dist} \sum_{k=0}^{\infty} rect\left(\frac{t - t_0}{\Delta_{dist}}\right)$$
$$\text{with } A_{dist} = \alpha_m \cdot T_{load}(t), \quad 0 < \alpha_m < 1$$
$$\text{and } t_0 = \frac{\Delta_{dist}}{2} + k \cdot T_{rect}. \tag{12}$$

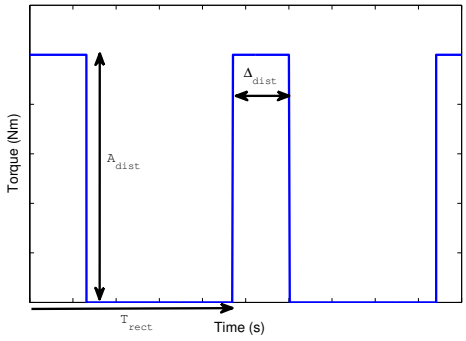

Fig. 2. Torque pulsation due to bearing damage.

α_m, the weighting of the damage related to the load torque, is set to 20%.

IV. Model validation

The developed model is evaluated and validated by measurements in the following. For this, the impact of the bearing damage on the stator current is investigated. The torque pulsations due to bearing damage cause speed fluctuations, which induce oscillations in the stator current with the frequency f_c. These are related to the electrical supply frequency f_{el} and the characteristic fault frequency f_{outer} from (5):

$$f_c = f_{el} \pm k \cdot f_{outer}. \quad k = 1, 2, 3, ... \tag{13}$$

For the measurements, a healthy and two cylindrical-roller bearings with artificial outer race fault are considered:

- the first damage is an artificial slot in the outer race with a width of $w_1 = 0.25\,\mathrm{mm}$.
- by the second damage, the outer race was wire eroded. The wire has a diameter of $8\,\mathrm{mm}$, which produces a damaged point in the outer race with a width of $w_2 = 2.8\,\mathrm{mm}$.

Considering the geometry of the bearing used and the number of balls given in Table V (Appendix B), the characteristic frequency of the outer race damage from (5) is reduced to

$$f_{outer} = \frac{N_{ball}}{2} \cdot f_{rm} \cdot (1 - \frac{D_{ball}}{D_{cage}}) = 4.25 \cdot f_{rm}, \tag{14}$$

because the contact angle β is $0°$ for cylindrical-roller bearing [17]. The number of the ball overruns through the damaged point is then $N_{outer} = 4.25$.

A. Simulation results

The developed model is evaluated for two damages respectively with the width of $w_1 = 0.25\,\mathrm{mm}$ and $w_2 = 2.8\,\mathrm{mm}$. The simulation is performed at a constant speed of $1500\,\mathrm{rpm}$ and a load torque of $0.1\,\mathrm{Nm}$. Thereby, the stator current and the torque of the machine are saved for the post-processing. To verify the proposed model, the stator current and the torque of the machine are spectrally analyzed. The expected characteristic frequencies f_c are calculated from (13) and the first eight values at $1500\,\mathrm{rpm}$ with $f_{el} = 100\,\mathrm{Hz}$ are summarized in table I.

TABLE I. Expected characteristic fault frequencies at 1500 rpm.

harmonic	Frequency ($k > 0$)[Hz]	Frequency ($k < 0$)[Hz]
$k = 1$	6.25	206.25
$k = 2$	112.5	312.5
$k = 3$	218.75	418.75
$k = 4$	325	525
$k = 5$	431.25	631.25
$k = 6$	537.5	737.5
$k = 7$	643.75	843.75
$k = 8$	750	950

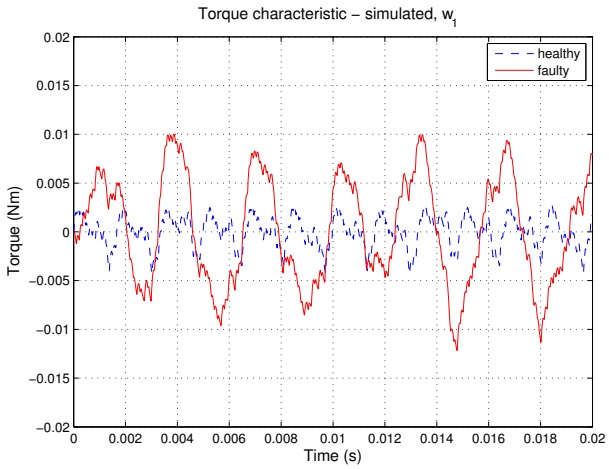

Fig. 3. Characteristic of the torque for w_1 at $1500\,\mathrm{rpm}$ and $0.1\,\mathrm{Nm}$.

The damage with the width w_1 is considered. Fig. 3 shows the characteristic of its simulated torque. Here, the constant component of the torque has been removed. When compared to the healthy case, a higher torque ripple is observed in the faulty one. The power spectral density (PSD) of the simulated torque is shown in Fig. 4. Seven characteristic frequencies: $6.25\,\mathrm{Hz}, 218.75\,\mathrm{Hz}, 312.5\,\mathrm{Hz}, 418.75\,\mathrm{Hz}, 525\,\mathrm{Hz}, 631.25\,\mathrm{Hz}$ and $737.5\,\mathrm{Hz}$ are clearly observed in the spectrum in the range of $0 - 750\,\mathrm{Hz}$. The amplitude of the characteristic frequencies $218.75\,\mathrm{Hz}, 312.5\,\mathrm{Hz}$ and $418.75\,\mathrm{Hz}$ is higher in comparison with all other harmonics. Furthermore, the current spectrum for the same damage is illustrated in Fig. 5, in which the characteristic fault frequencies present in the spectrum are marked. All of the visible frequencies are present in the torque spectrum in the range of $750\,\mathrm{Hz}$. The higher amplitude are present at: $6.25\,\mathrm{Hz}, 218.75\,\mathrm{Hz}, 312.5\,\mathrm{Hz}$ and $418.75\,\mathrm{Hz}$. The faulty case is clearly distinguished from the healthy one.

In order to illustrate the effect of the damage size, the damage with the width of $w_2 = 2.8\,\mathrm{mm}$ is analyzed. As depicted in the torque spectrum in Fig. 6, the characteristic fault frequencies are more pronounced than for the damage with w_1.

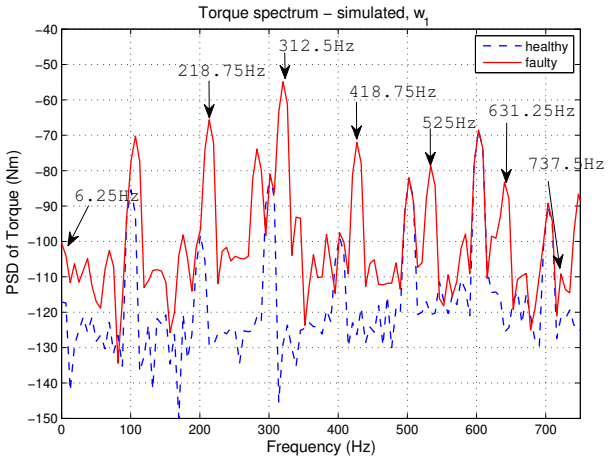

Fig. 4. PSD of the torque for w_1 at $1500\,\mathrm{rpm}$ and $0.1\,\mathrm{Nm}$.

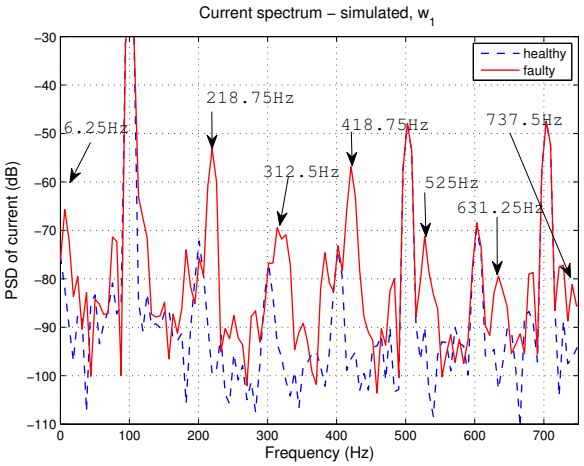

Fig. 5. PSD of the current for w_1 at 1500 rpm and 0.1 Nm.

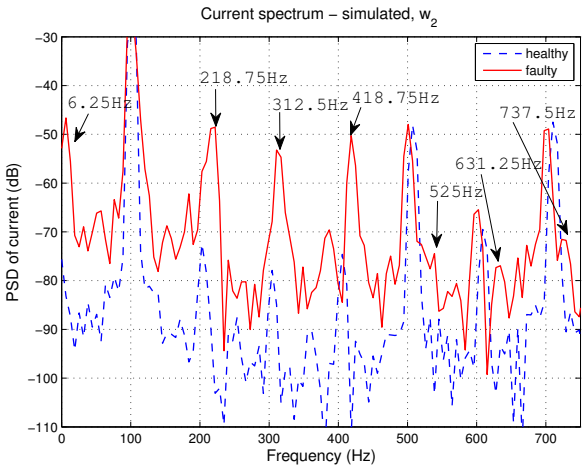

Fig. 7. PSD of the current for w_2 at 1500 rpm and 0.1 Nm.

The same behavior is observed in the current spectrum shown on Fig. 7, in which the frequency of 6.25 Hz and 312.5 Hz are better visible. Table II summarizes the characteristic frequencies, which appear in the current spectrum for a better comparison. The developed model represents the impact of bearing damage on the stator current, so that the faulty case can clearly be differentiated from the healthy one.

B. Experimental results

A test bench of the PMSM are used to validate the proposed approach. This consists of a vector-controlled PMSM, a load machine and a cylindrical-roller bearing in a special test bench housing. The rated data of the machine are given in Table V (Appendix B). The bearing housing is connected to the motor and the load by shaft couplings. The load torque is measured by a torque transducer, which is placed between the motor and the bearing housing. The sampling rate frequency for the current measurement is 100 kHz, while it is 20 kHz for the torque measurement. Moreover, the measured current is filtered by a second-order butterworth filter with a cutoff-frequency of 12.5 Hz. The measured data were collected by means of the National Instruments measurement system NI PXIe-8133. For the verification, three bearings are used during the experiment: a healthy bearing and two bearing damages described in section IV-A above. These damages have a similar size compared to the simulated damages. The motor is driven with the same parameters as in the simulation: a constant speed of 1500 rpm and a load torque of 0.1 Nm. The current and the torque are measured for both damages and spectrally analyzed.

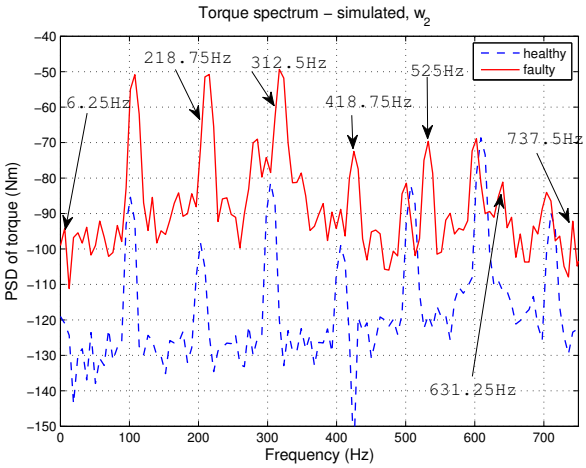

Fig. 6. PSD of the torque for w_2 at 1500 rpm and 0.1 Nm.

Fig. 8 shows the torque characteristic for the damage with the width of $w_1 = 0.25$ mm, whose constant component is removed for the comparison with the simulated characteristic. The characteristic shows a rise of the amplitude and the occurrence of torque ripple in the faulty case. When compared to the simulation results, the amplitude is higher. Additionally, several characteristic fault frequencies due to the outer race fault are present in the spectrum of the measured torque in Fig. 9. These frequencies are 418.75 Hz, 525 Hz, 631.25 Hz and 737.5 Hz. The spectral analysis of the current for the same damage is shown in Fig. 10, in which the characteristic frequencies are marked. The amplitude of the present characteristic fault frequencies can be distinguished from the healthy case in spite the fact that they are small in comparison with the amplitude of other present frequencies. E.g. the frequency 431.25 Hz occurs with an amplitude closed to the noise amplitude, while the frequency 631.25 Hz appear with an amplitude of +7.80 dB in comparison to the healthy bearing.

The stronger damage with the width of $w_2 = 2.8$ mm is now analyzed. Fig. 11 illustrates the spectrum of the measured current for the damage with w_2. The present characteristic

TABLE II. COMPARISON OF THE CHARACTERISTIC FREQUENCIES AT DIFFERENT FAULT CONDITIONS FOR SIMULATION RESULTS.

Frequency	Healthy	Faulty (w_1)	Faulty (w_2)
6.25 Hz	-82.03 dB	-65.72 dB	-46.63 dB
218.75 Hz	-98.62 dB	-53.18 dB	-48.5 dB
312.5 Hz	-93.52 dB	-69.46 dB	-53.22 dB
418.75 Hz	-96.53 dB	-56.86 dB	-50.28 dB
525 Hz	-90.03 dB	-71.25 dB	-74.48 dB
631.25 Hz	-102.7 dB	-79.42 dB	-77.34 dB
737.5 Hz	-90.02 dB	-77.21 dB	-71.75 dB

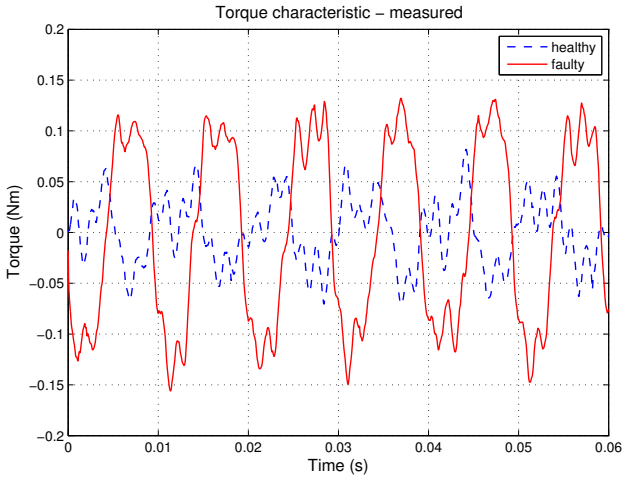

Fig. 8. Measured characteristic of the torque for w_1 at 1500 rpm and 0.1 Nm.

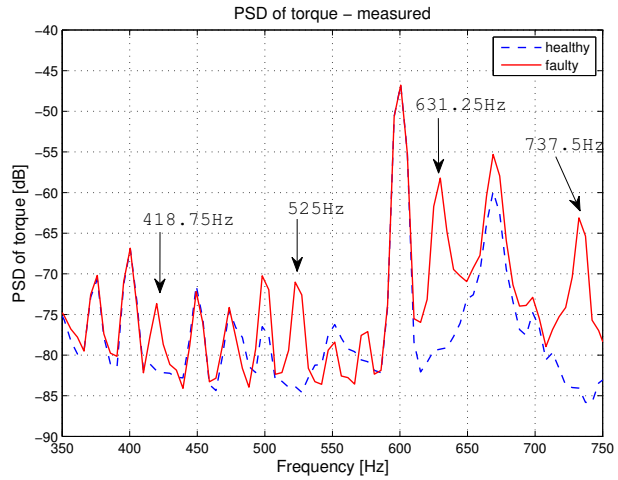

Fig. 9. PSD of the measured torque for w_1 at 1500 rpm and 0.1 Nm.

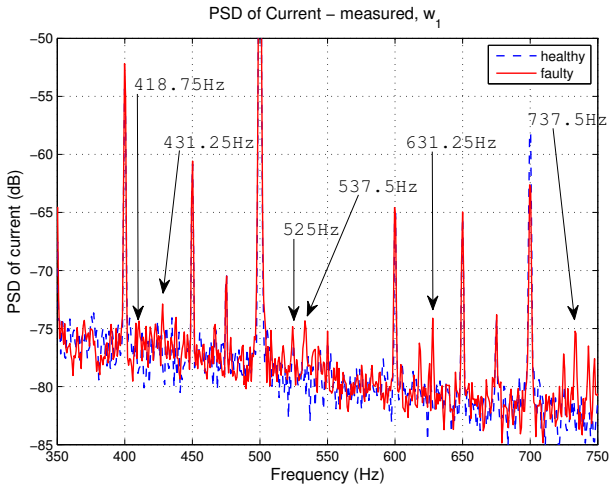

Fig. 10. PSD of the measured current for w_1 at 1500 rpm and 0.1 Nm.

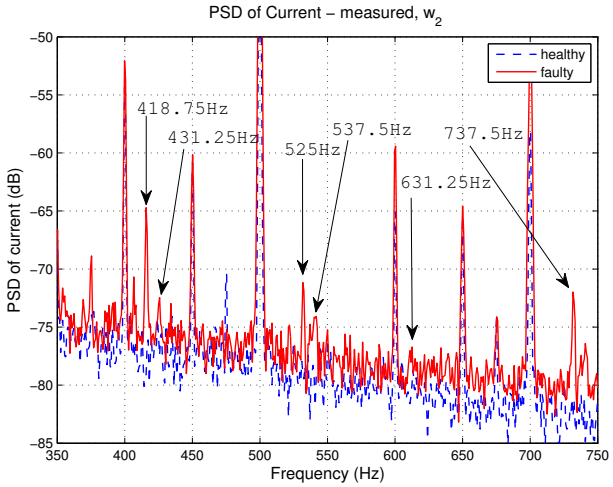

Fig. 11. PSD of the measured current for w_2 at 1500 rpm and 0.1 Nm.

frequencies are better visible as in the first damage excepted at 631.25 Hz, in which the amplitude is closed to the noise amplitude. However, the frequency 418.75 Hz appears with a deviation of +14.6 dB, when compared to the healthy bearing as shows the table III, which summarizes the characteristic frequencies present in the measured current spectrum.
Despite the fact that not always the same frequencies are generated, the characteristic frequencies appear in the simulated as well as in the measured current spectrum. The proposed approach represents clearly the effect of the bearing damage in the current and the torque of the PMSM.

V. Conclusion

A model of a PMSM considering the effects of bearing damage has been developed. For this purpose, the disturbing torque due to bearing damage has been implemented and superposed with the load torque in the PMSM. The proposed approach has been simulated for different damages and verified by measurements. For the verification, the current and the torque were spectrally analyzed. Several characteristic fault frequencies occur in the spectrum of the simulated current and torque. A strong damage in the outer race can easier be distinguished than a small one. The comparison between the simulated and the measured results has clearly demonstrated the accuracy of the proposed approach. However, not always the same fault frequencies occur in the spectrum of the simulations as well as in the measurements. The developed model represents the impact of the damaged bearing on the torque and the current, in such a way that the generated simulation data can be used to implement fault detection and

TABLE III. Comparison of the characteristic frequencies at different fault conditions for the measurements

Frequency	healthy	faulty (w_1)	faulty (w_2)
418.75 Hz	-79.32 dB	-74.80 dB	-64.72 dB
431.25 Hz	-77.27 dB	-74.04 dB	-72.58 dB
525 Hz	-79.17 dB	-74.83 dB	-74.25 dB
537.5 Hz	-79.47 dB	-74.34 dB	-71.16 dB
631.25 Hz	-81.90 dB	-74.11 dB	-76.79 dB
737.5 Hz	-81.26 dB	-75.45 dB	-71.98 dB

classification algorithms.

APPENDIX A
DATA OF THE USED CYLINDRICAL-ROLLER BEARING.

TABLE IV. DATA OF THE USED CYLINDRICAL-ROLLER BEARING.

	N203E-TVP2
inner diameter d	$17\,\mathrm{mm}$
outer diameter D	$40\,\mathrm{mm}$
roller diameter D_{ball}	$6.5\,\mathrm{mm}$
cage diameter D_{cage}	$28.6\,\mathrm{mm}$
raceway groove radius r_a	$17.55\,\mathrm{mm}$
number of balls/rollers N_{ball}	11

APPENDIX B
DATA OF THE USED MACHINE (RATED VALUES).

TABLE V. DATA OF THE USED MACHINE (RATED VALUES).

	PMSM
power	$500\,\mathrm{W}$
pole pair	4
current	$2.3\,\mathrm{A}$
speed	$3000\,\mathrm{min}^{-1}$
torque	$1.6\,\mathrm{Nm}$
moment of inertia	$0.4239\,\mathrm{kgcm}^2$
direct inductance L_{sd}	$28.6\,\mathrm{mH}$
quadrature inductance L_{sq}	$31.6\,\mathrm{mH}$
resistance R_s at $20^\circ C$	$5.6\,\Omega$

REFERENCES

[1] A. H. Bonnett and C. Yung, "Increased Efficiency Versus Increased Reliability", Industry Applications Magazine, IEEE, vol. 14, no. 1, pp. 29 - 36, January - February 2008.

[2] P. F. Albrecht , J. C. Appiarius , R. M. McCoy, E. L. Owen and D. K. Sharma, "Assessment of the reliability of motors in utility applications - updated", IEEE Transactions on Energy Conversion, vol. EC-1, no. 1, pp. 39 - 46, 1986.

[3] I. Bediaga, X. Mendizabal,A. Arnaiz and J. Munoa, "Ball bearing damage detection using traditional signal processing algorithms," Instrumentation & Measurement Magazine, IEEE, vol. 16, no. 2, pp. 20 - 25, April 2013.

[4] R. R. Schoen, T. G. Habetler, F. Kamran and R. G. Bartheld, "Motor bearing damage detection using stator current monitoring," IEEE Transactions on Industry Applications, vol. 31, no. 6, pp. 1274 - 1279, November - December 1995.

[5] B. M. Ebrahimi, J. Faiz, J. and B. N. Araabi, "Pattern identification for eccentricity fault diagnosis in permanent magnet synchronous motors using stator current monitoring," Electric Power Applications, IET, vol. 4, no. 6, pp. 418 - 430, July 2010.

[6] S. Nandi, H. A. Toliyat and L. Xiaodong, "Condition monitoring and fault diagnosis of electrical motors-a review," IEEE Transactions on Energy Conversion, vol. 20, no. 4, pp. 719-729, December 2005.

[7] M. Pacas, S. Villwock and R. Dietrich, "Bearing damage detection in permanent magnet synchronous machines," Energy Conversion Congress and Exposition, ECCE 2009, IEEE, pp. 1098 - 1103, September 2009.

[8] R. Obaid, T. Habetler and J. Stack, "Stator current analysis for bearing damage detection in induction motors," 4th IEEE International Symposium on Diagnostics for Electric Machines, Power Electronics and Drives, SDEMPED 2003, pp. 182 - 187, 2003.

[9] Z. Obeid, S. Poignant, J. Regnier and P. Maussion, "Stator current based indicators for bearing fault detection in synchronous machine by statistical frequency selection," IECON 2011 - 37th Annual Conference on IEEE Industrial Electronics Society, pp. 2036 - 2041, 2011.

[10] M. Blödt, P. Granjon, B. Raison and G. Rostaing, "Models for Bearing Damage Detection in Induction Motors Using Stator Current Monitoring, " IEEE Trans. on Industrial Electronics, vol. 55, no. 4, pp. 1813 - 1822, April 2008.

[11] A. Picot, Z. Obeid, J. Regnier, P. Maussion, S. Poignant and O. Darnis, "Bearing fault detection in synchronous machine based on the statistical analysis of stator current," IECON 2012 - 38th Annual Conference on IEEE Industrial Electronics Society, pp. 3862 - 3867, 2012.

[12] M. Blödt, J. Faucher, B. Dagues and M. Chabert, "Mechanical load fault detection in induction motors by stator current time-frequency analysis," IEEE International Conference on Electric Machines and Drives, pp. 1881-1888, 2005.

[13] Jaehoon Kim, Inseok Yang, Donggil Kim, M. Hamadache and Dongik Lee, "Bearing fault effect on induction motor stator current modeling based on torque variations," 12th International Conference on Control, Automation and Systems 2012 (ICCAS), pp. 814 - 818, 17-21 October 2012.

[14] A. Rezig, A. N'Diaye, M. R. Mekideche and A. Djerdir, "Modelling and detection of bearing faults in Permanent Magnet Synchronous Motors," XXth International Conference on Electrical Machines (ICEM 2012), pp. 1778 - 1782, 2012.

[15] J. Stack, T. Habetler and R. Harley, "Fault classification and fault signature production for rolling element bearings in electric machines," 4th IEEE International Symposium on Diagnostics for Electric Machines, Power Electronics and Drives, SDEMPED 2003, pp. 172 - 176, 24-26 August 2003.

[16] T. Herold, D. Franck, L. Enno and K. Hameyer, "Extension of a d-q model of a permanent magnet excited synchronous machine by including saturation, cross-coupling and slotting effects," Electric Machines and Drives Conference (IEMDC), 2011 IEEE International, pp. 1363 - 1367, 15-18 May 2011.

[17] P. Tavner, L. Ran, J. Penman and H. Sedding, "Condition monitoring of rotating electrical machines," IET Power and Energy Series, 56, 2008.

[18] Tedric. A. Harris, Roller bearings analysis, John Wiley & Sons, New York, 2001.

Christelle Piantsop Mbo'o was born in 1982 in Douala, Cameroon. She received her Dipl.-Ing. degree in electrical engineering in 2008 from RWTH Aachen University, Germany. Since 2009 she has been a researcher at the Institute of Electrical Machines (IEM). Her research interests include analysis and design of electrical machines.

Dr. Kay Hameyer (FIET, SMIEEE) received his M.Sc. degree in electrical engineering from the University of Hannover and his Ph.D. degree from the Berlin University of Technology, Germany. After his university studies he worked with the Robert Bosch GmbH in Stuttgart, Germany as a Design Engineer for permanent magnet servo motors and vehicle board net components. Until 2004 Dr. Hameyer was a full Professor for Numerical Field Computations and Electrical Machines with the KU Leuven in Belgium. Since 2004, he is full professor and the director of the Institute of Electrical Machines (IEM) at RWTH Aachen University in Germany. 2006 he was vice dean of the faculty and from 2007 to 2009 he was the dean of the faculty of Electrical Engineering and Information Technology of RWTH Aachen University. His research interests are numerical field computation and optimization, the design and controls of electrical machines, in particular permanent magnet excited machines, induction machines and the design employing the methodology of virtual reality. Since several years Dr. Hameyer's work is concerned with the development of magnetic levitation for drive systems, magnetically excited audible noise in electrical machines and the characterization of ferro-magnetic materials. Dr. Hameyer is author of more then 250 journal publications, more then 500 international conference publications and author of 4 books. Dr. Hameyer is a member of VDE, IEEE senior member, fellow of the IET.